Supporting Information

Structural Transformation of Selenidostannates from 1D to 0D and 2D *via* Stepwise Amine-Templated Assembly Strategy

Dandan Hu,‡ Yingying Zhang,‡ Huajun Yang, Jian Lin, and Tao Wu*

College of Chemistry, Chemical Engineering and Materials Science, Soochow University, Suzhou, Jiangsu 215123, China

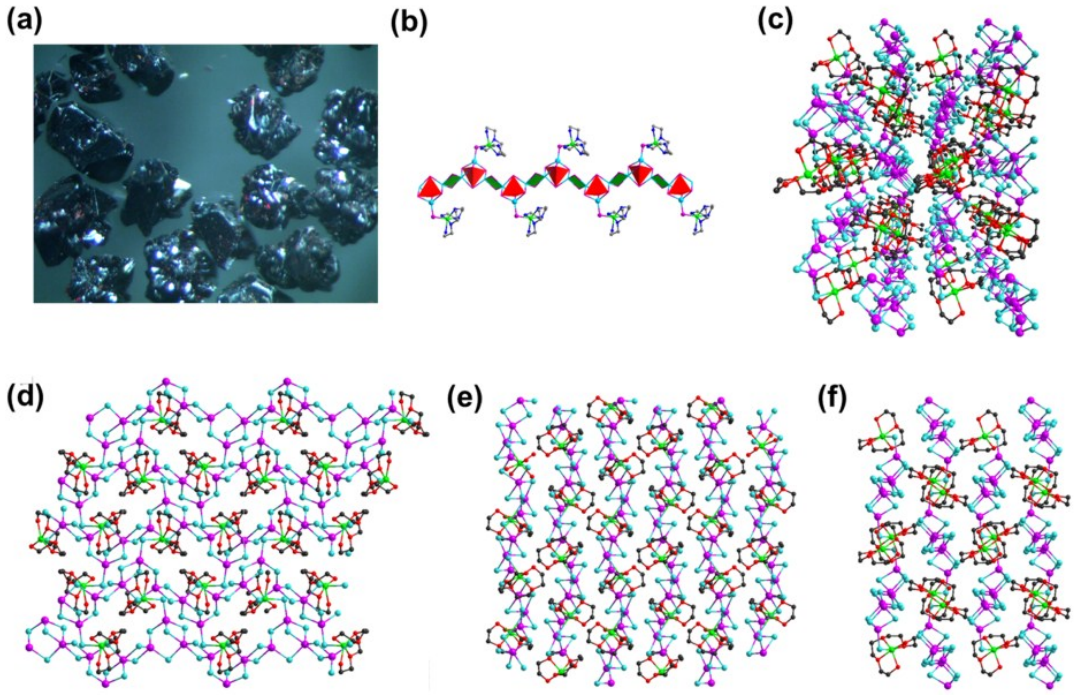

Fig. S1 (a) Crystal morphology of **1**; (b) 1D chain unit of $[Sn_3Se_7Fe(TEPA)]_n$; (c-d) the packing diagram viewed along crystal unit axis.

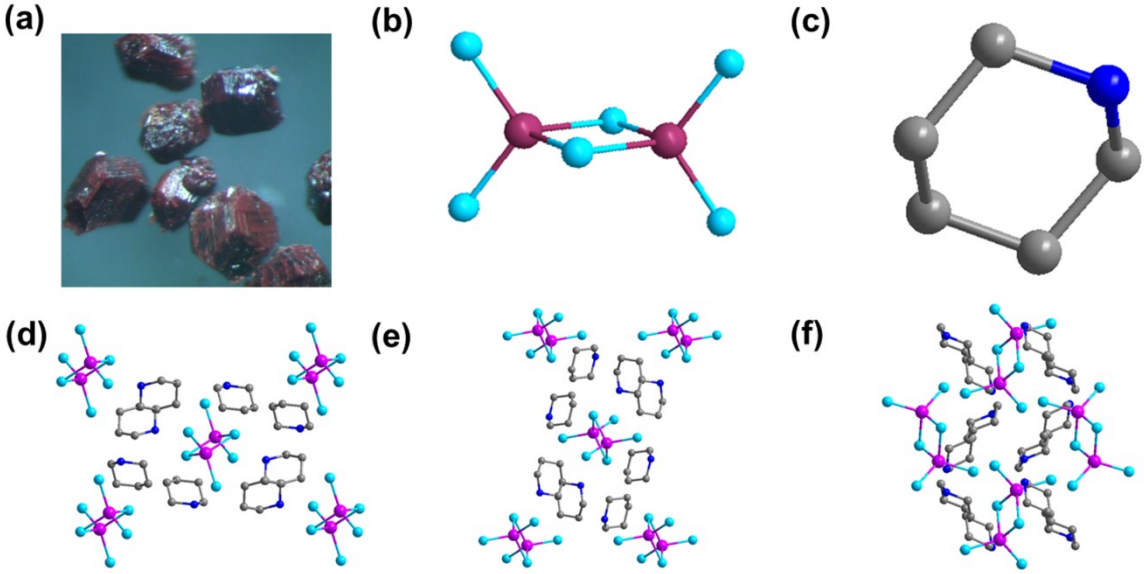

Fig. S2 (a) The transmission pattern of 0D $[Sn_2Se_6]\cdot4(H^+\text{-PR})$ dimer crystal morphology; (b) the structure of $Sn_2Se_6^{4-}$ dimer; (c) the counter ions, namely $2(H^+\text{-PR})$; (d) packing mode of the $Sn_2Se_6^{4-}$ dimer crystal viewed along a axis; (e) packing mode of the $Sn_2Se_6^{4-}$ dimer crystal viewed along b axis; (f) packing mode of the $Sn_2Se_6^{4-}$ dimer crystal viewed along c axis.

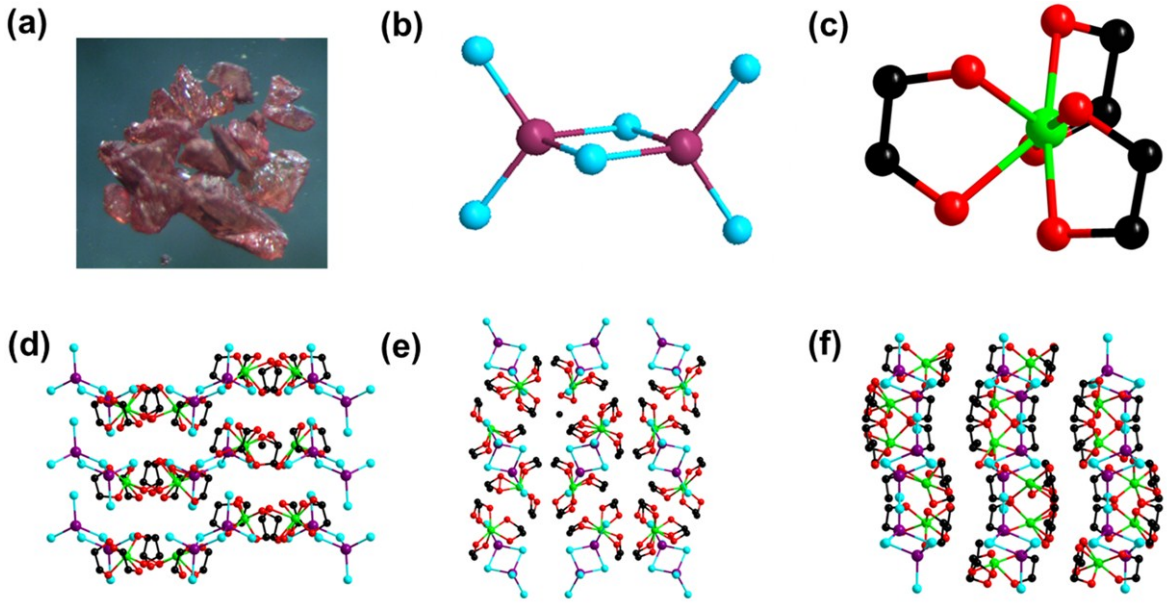

Fig. S3 (a) The transmission pattern of 0D $[Sn_2Se_6]\cdot 2[Fe(en)_3]$ dimer crystal morphology; (b) the structure of $Sn_2Se_6^{4-}$ dimer; (c) the counter ions, namely $[Fe(en)_3]^{2+}$; (d) packing mode of the $Sn_2Se_6^{4-}$ dimer crystal viewed along a axis; (e) packing mode of the $Sn_2Se_6^{4-}$ dimer crystal viewed along *b* axis; (f) packing mode of the $Sn_2Se_6^{4-}$ dimer crystal viewed along c axis.

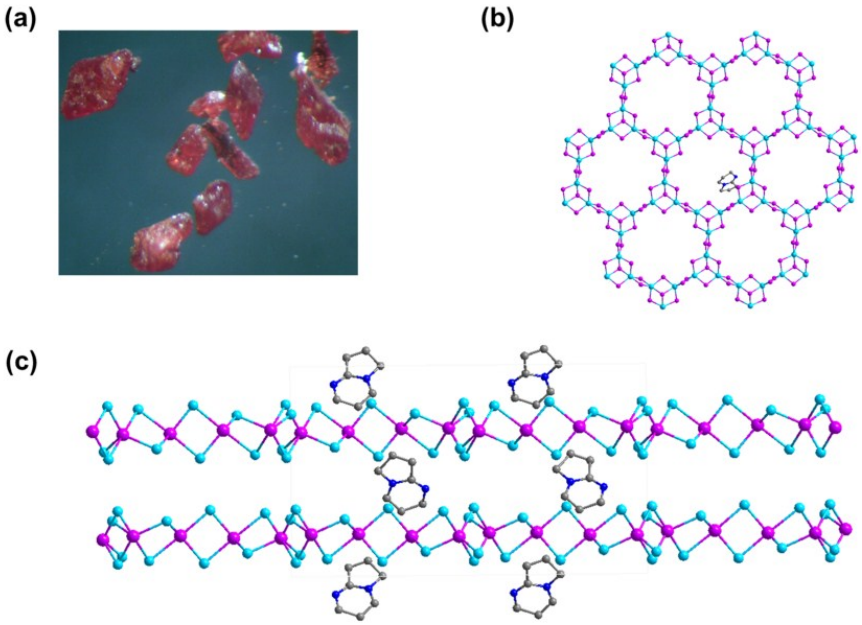

Fig. S4 (a) Crystal morphology of **4**; (b) 2D layer; (c) packing mode of the 2D $[Sn_3Se_7]_n\cdot 2n(H^+\text{-DBN})$ layer crystal viewed along b axis. 2D $[Sn_3Se_7]_n\cdot 2n(H^+\text{-DBN})$ layer possess a famous 6 net $[Sn_3Se_7]_n^{2n-}$ lamellar structure with protonated DBN located in the inter-layer spaces. The lamellar $[Sn_3Se_7]_n^{2n-}$ anion could be viewed as consisted by the $[Sn_3Se_7]_n^{2n-}$ single chains linked the adjacent $[Sn_3Se_7]_n^{2n-}$ chains through the terminal Se atoms of the $SnSe_4$ tetrahedral. And, the $[Sn_3Se_7]$ units are interconnected with each other by edge-sharing two Se atoms forming an chain.

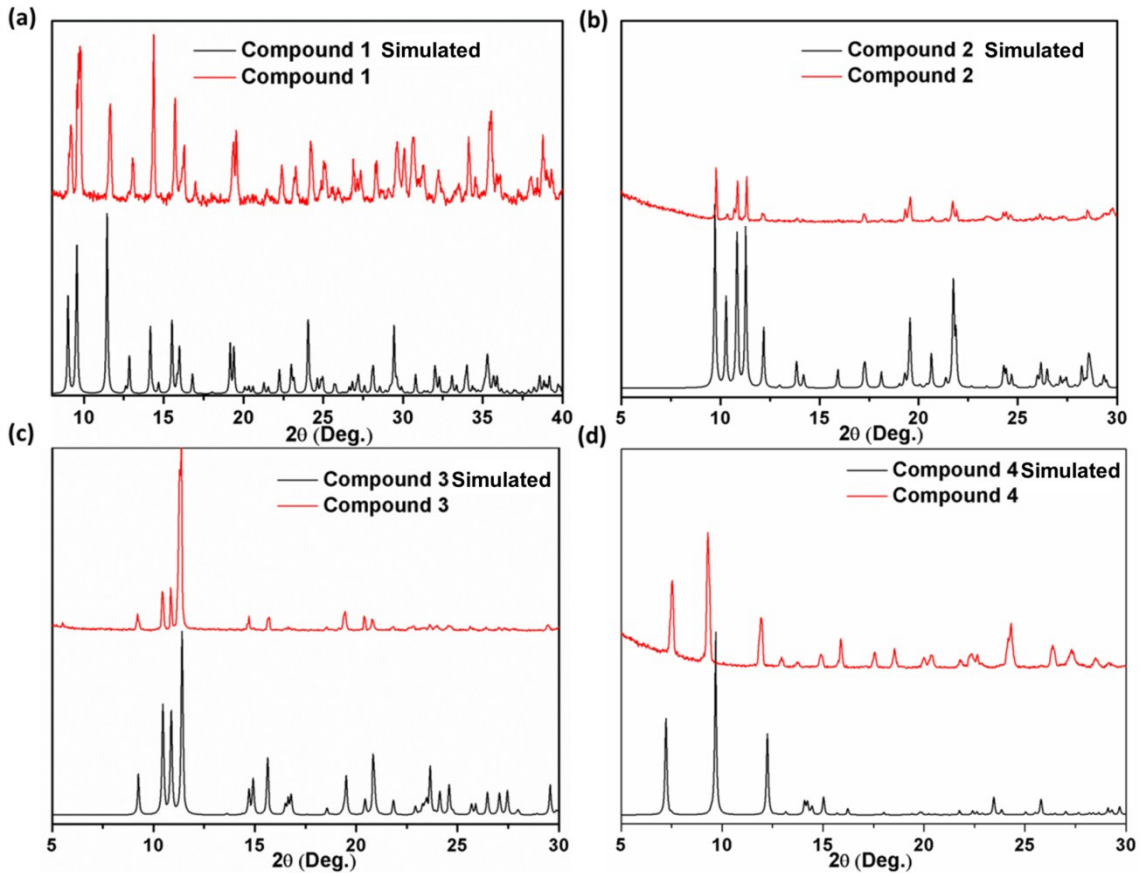

Fig. S5 The simulated and experimental PXRD patterns of compound **1-4**.

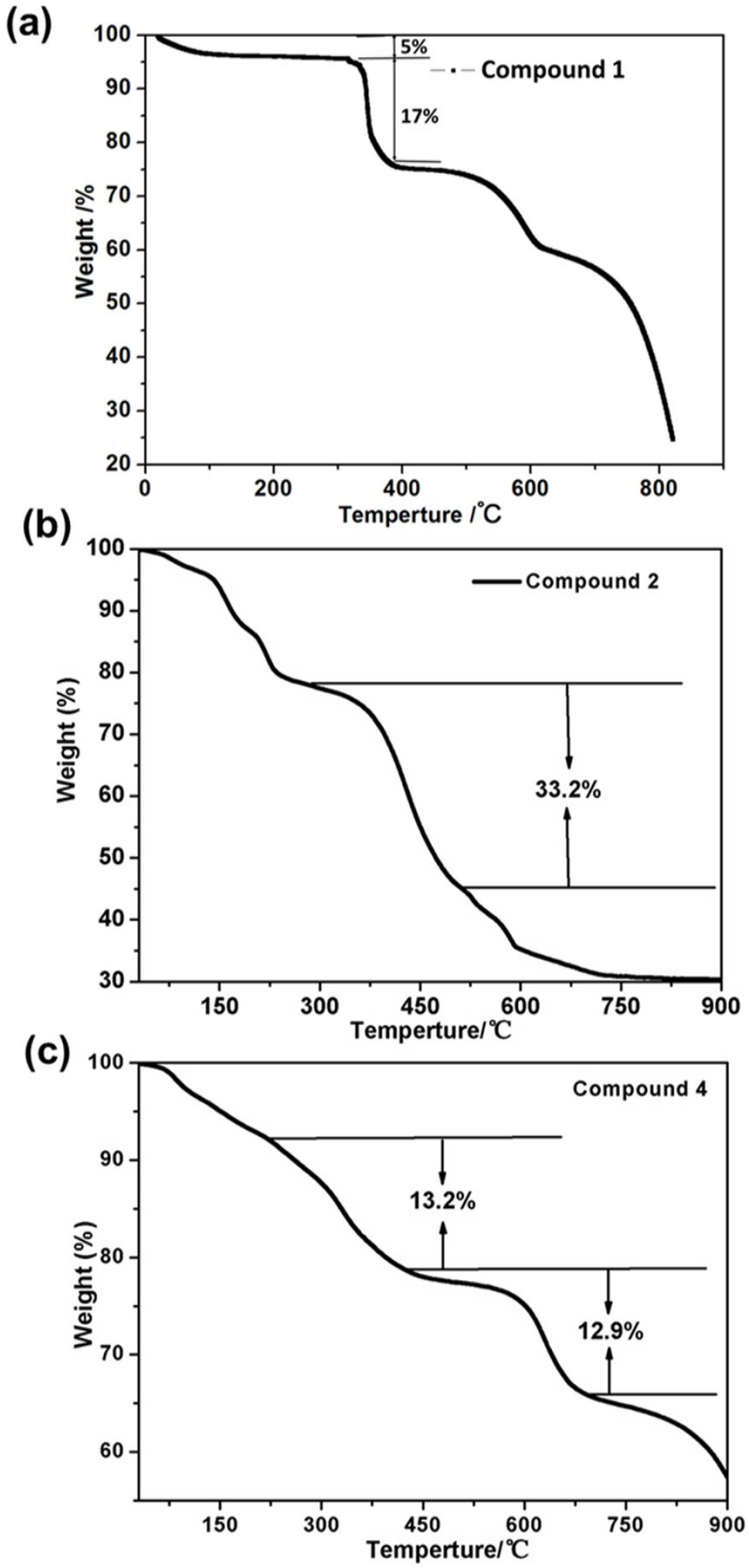

Fig. S6 TGA curve for compound **1, 2 and 4**.

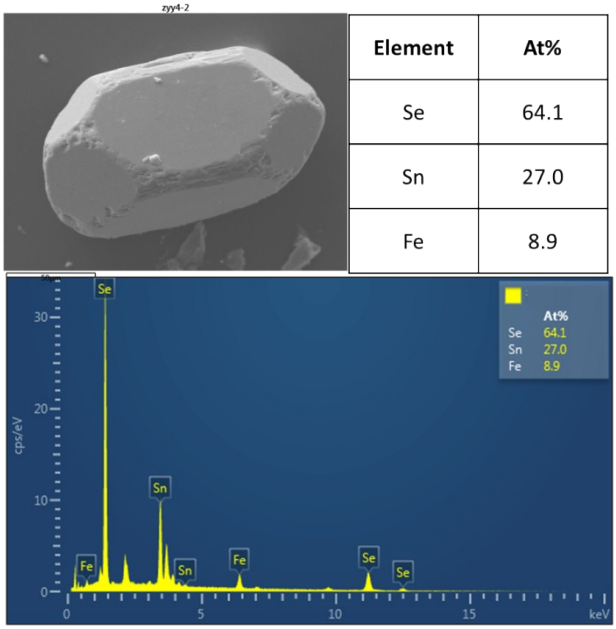

Fig. S7 EDX spectrum of compound **1**.

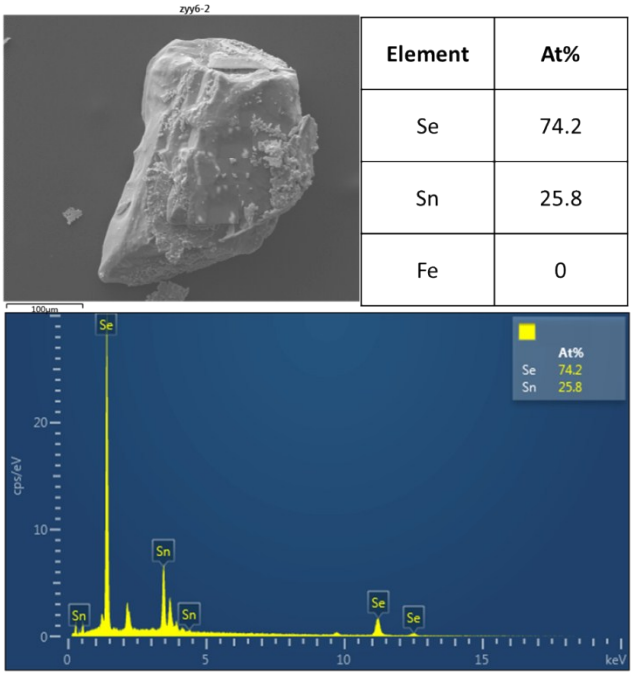

Fig. S8 EDX spectrum of compound **2**.

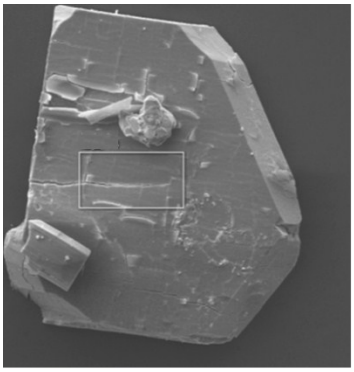

Element	At%
Se	60.6
Sn	20.5
Fe	18.9

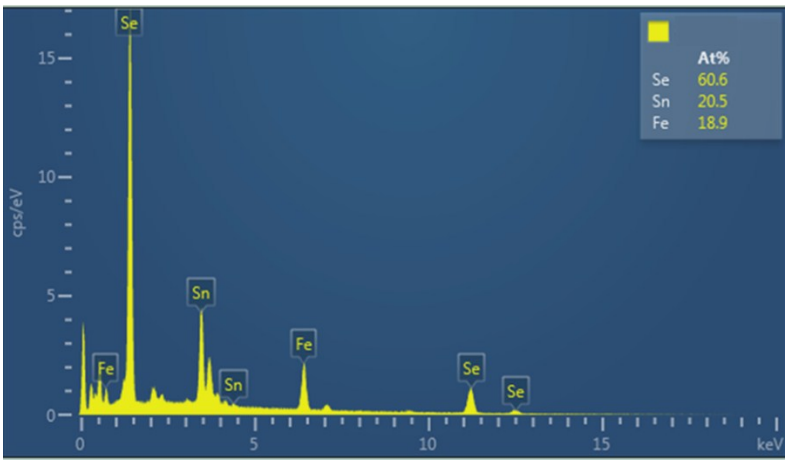

Fig. S9 EDX spectrum of compound **3**.

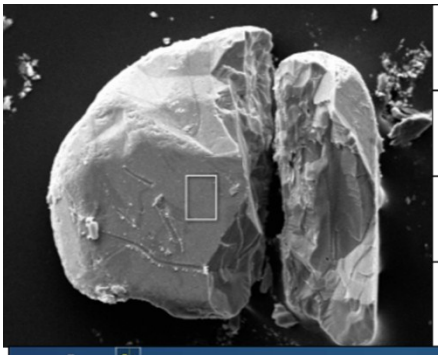

Element	At%
Se	69.1
Sn	30.9
Fe	0

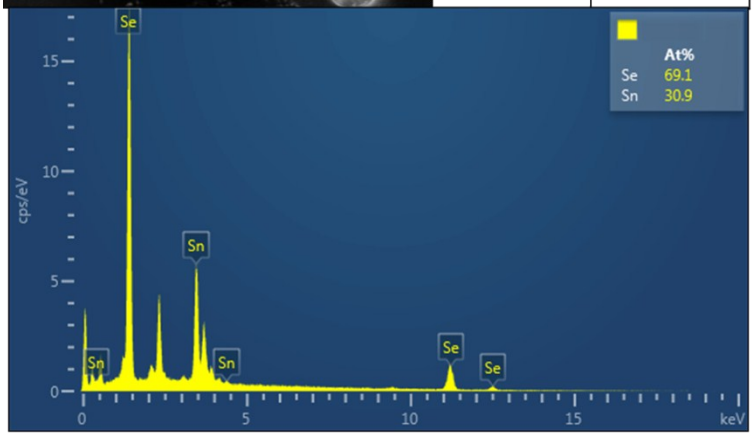

Fig. S10 EDX spectrum of compound **4**.

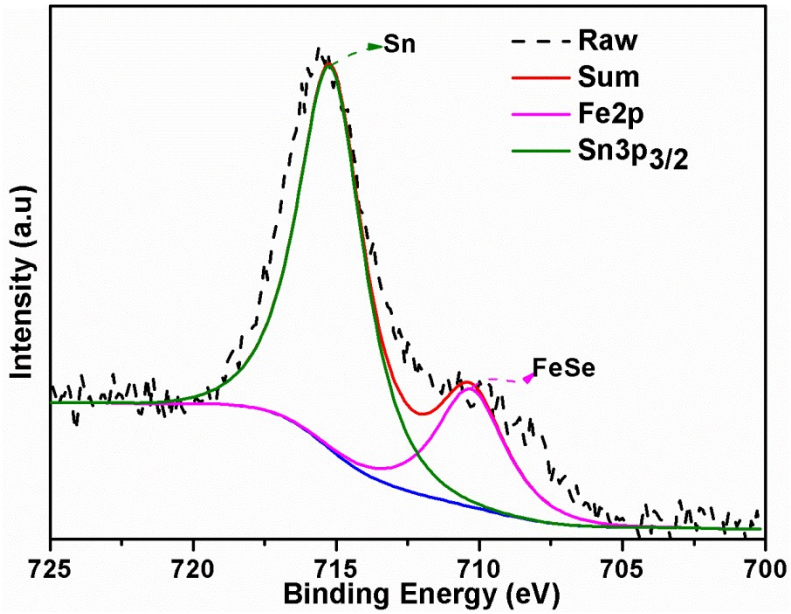

Fig. S11 The X-ray photoelectron spectroscopy (XPS) of compound **1**.

Table S1 Crystal Data and Structure Refinement Parameters for Compound 1-4.

Compound	**1**	**2**	**3**	**4**
Formula	$[Sn_3Se_7Fe(TEPA)]$	$[Sn_2Se_6]\cdot4(H^+$-PR)	$[Sn_2Se_6]\cdot2[Fe(en)_3]$	$[Sn_3Se_7]\cdot2(H^+$-DBN)
Crystal system	Orthorhombic	Monoclinic	Orthorhombic	Orthorhombic
Z	4	2	8	2
Space group	$P2_12_12_1$	$P2_1/n$	$Pbca$	$Cmc2_1$
cell (Å)	a = 12.4953(3) b = 13.7745(3) c = 14.0233(3)	a = 10.3277(4) b = 10.2808(4) c = 15.7823(6)	a = 15.5062(9) b = 11.8662(7) c = 19.0966(11)	a = 13.4435(4) b = 24.4817(6) c = 14.4494(4)
β (deg.)	90	96.725(4)	90	90
V (Å^3)	2143.74(9)	1664.19(11)	3513.8	4083.76
D (g cm^{-3})	3.112	2.0110	2.146	2.852
μ (mm^{-1})	14.215	8.075	8.450	13.831
$2\theta_{max}$ (deg.)	39.4670	31.027	27.562	90.946
GOF on F^2	1.064	1.088	1.042	1.176
R_1, wR_2 ($I>2\sigma(I)$)	0.0434, 0.0998	0.0429, 0.1140	0.0517, 0.1290	0.0365, 0.1119
R_1, wR_2 (all data)	0.0474, 0.1025	0.0585, 0.1264	0.0743, 0.1469	0.0491, 0.1238